Triggering of Buneman instability and existence of multiple double layers in laboratory plasma

Article *in* Physics Letters A · September 2017

DOI: 10.1016/j.physleta.2017.09.022

3 authors, including:

Prince Alex
Università degli Studi di Milano-Bicocca
10 PUBLICATIONS **10** CITATIONS
SEE PROFILE

Kumar Sinha Suraj
Pondicherry University
22 PUBLICATIONS **77** CITATIONS
SEE PROFILE

Physics Letters A 381 (2017) 3652–3658

Contents lists available at ScienceDirect

Physics Letters A

www.elsevier.com/locate/pla

Triggering of Buneman instability and existence of multiple double layers in laboratory plasma

Prince Alex *, Saravanan Arumugham, Suraj Kumar Sinha

Department of Physics, School of Physical Chemical and Applied Sciences, Pondicherry University, Pudhucherry, Kalapet, 605014, India

ARTICLE INFO

Article history:
Received 10 March 2017
Received in revised form 15 August 2017
Accepted 12 September 2017
Available online 14 September 2017
Communicated by F. Porcelli

Keywords:
Glow discharge plasma
Double layer
Buneman instability
Floating potential
Aurora

ABSTRACT

We report experimentally observed triggering criteria for Buneman instability and boundary conditions for existence of multiple double layers (MADL) in glow discharge plasma. The MADLs are generated by accelerating plasma electrons towards a positively biased electrode submerged in it. The boundary conditions for the formation and existence of MADL are obtained from the experiment in terms of electron drift velocity (v_d) and electron thermal velocity (v_{te}). The MADL is found to exist within the range $3v_{te} \geq v_d \geq 1.3v_{te}$. For the condition $v_d \geq 1.3v_{te}$, rise of an instability and simultaneous formation of MADL is observed in the experiment. The analysis of fluctuations in floating potential showed that the instability has all the characteristics of Buneman instability.

1. Introduction

Double layers (DLs) in plasma represents a non-neutral region of opposite charges separated by a small distance with a potential drop of the order of $|\phi_0| \geq kT/e$ across the layer [1]. They are suggested to be responsible for energizing auroral particles in ionosphere, solar flares, acceleration of charged particles in space plasma etc. The investigation on DL are frequently reported in space plasma [2–7], numerical simulation [8–12], theoretical plasma study [13–16] and also in a series of different types of laboratory plasma devices [17–20]. In addition, DLs have received enormous interest in the recent past because of its interdisciplinary nature and are known to play significant role in electrochemical super-capacitors [21], biological systems such as amphiphilic bilayers [22], heterogeneous fluid-based systems such as blood [23], paint etc. In laboratory, DL is generally produced by applying a potential drop or passing a current through plasma or by injecting an electron beam into plasma which often leads to current driven or beam related instabilities. Singh and Schunk, in a numerical simulation relevant to auroral plasma, showed the recurring formation of moving DL in a current driven plasma and demonstrated the role of Buneman instability in the reformation process through one dimensional model [24]. Studies carried out by Smith and Goertz [25] shows that excitation condition for Buneman instability exactly match with the Bohm criteria, i.e., $v_d \geq 1.3v_{te}$ where v_d is the electron drift velocity and v_{te} is the electron thermal velocity. In this article, we present experimental results from MADL, an experimental analog of auroral DL. Results clearly demonstrate, for the first time experimentally, that the triggering of Buneman instability leads to formation of MADL in the present experimental conditions. Our results are closely matching with findings of numerically simulated double layers in auroral plasma by Singh et al. [24].

The MADL in the present investigation consisting of more than one concentric layers and are generated by accelerating plasma electrons towards a positively biased electrode submerged in it. Analysis of satellite data by Temerin et al. [26] suggested that in auroral region, electrons are accelerated to large energies by a multiple double layer comprised of a series of many DL, rather than by a single DL. Computer simulations [27] also produced such a series of DLs, which somewhat resemble the proposed auroral structure. Bailey et al. demonstrated experimentally that a multistep DL or multiple DL (MDL) structure resembles very much to those data inferred from satellite measurements of auroral DL [28–31]. The understanding of DL in auroral region was greatly aided by Viking [32], S3-3 [33] and FAST [34] satellite including observation of parallel electric field, characterization of downward current region by electron drifting in the anti-earthward direction etc. But the issues concerning the formation and existence condition, relevance of instability in DL dynamics are far from complete. Also in space one is often limited to remote observations or data from a single pass of a spacecraft from which it might be difficult to even distinguish between spatial and temporal variations. Due to these reasons+

* Corresponding author.
E-mail address: princealexanderm@gmail.com (P. Alex).

http://dx.doi.org/10.1016/j.physleta.2017.09.022
0375-9601/

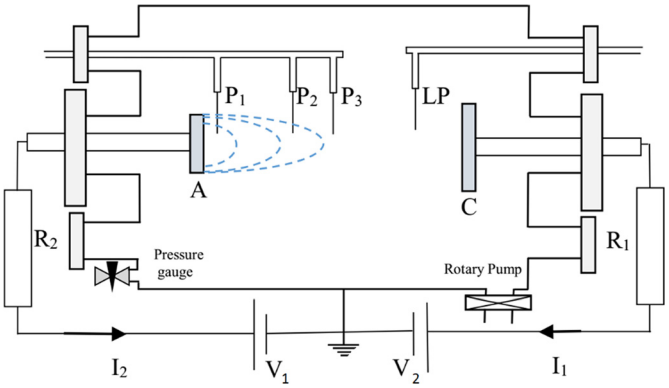

Fig. 1. Schematic of the experimental setup. A typical ADL profile with concentric DL structure is schematically shown in front of the anode. V_1 and V_2 = DC power supplies, A = anode, C = cathode, R_1 and R_2 = current limiting resistor, I_1 and I_2 = current measured through R_1 and R_2. P_1, P_2 and P_3 = floating probes. P_L = Langmuir probe.

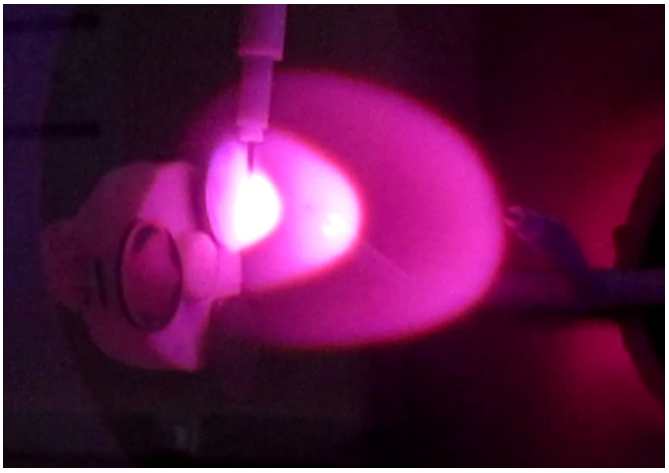

Fig. 2. (Multimedia view), experimental observation of multiple anodic double layer consisting of three layers at 0.2 mbar pressure.

MADL in the present investigation can be used as a testbed for studying auroral DL. The study provides the experimental boundary condition for the formation and existence of MADL obtained in terms of drift velocity and discharge parameters. The requirement of drift velocity condition gives rise to a lower limit for the formation of MADL which is consistent with Buneman instability condition, $v_d \geq 1.3v_{te}$. We have obtained an experimental upper limit, at which DL vanishes. The obtained upper limit is in agreement with the condition, $v_d \geq 3v_{te}$, given by Quon and Wong for ordinary simple DL produced in double plasma machine [35]. The time dependent floating potential fluctuations, obtained using floating probes, showed the excitation and growth of an instability with features similar to that of nonlinear evolution of Buneman instability [36].

The findings of the present investigation, mainly the condition for triggering Buneman instability and existence of MADL, provide a fundamental understanding of DLs. These results can be extended to improve the understanding of basic governing processes of DLs in space science, astrophysical system, solar corona, supercapacitors, biological system etc.

2. Experimental setup and generation of MADL

The experiment was performed in a modified dc glow discharge plasma set-up as shown in Fig. 1. Two disk shaped electrodes made of iron (Fe) and tungsten (W) used as cathode and anode respectively and are kept at a distance of 300 mm from each other. A high voltage DC power supply V_1 was used for application of negative bias up to -1 kV between cathode C and the grounded chamber. Another DC power supply V_2 was used for application of positive bias on anode in the range of 0–200 V. Two current limiting resistors, R_1 (100 Ω) and R_2 (100 Ω) were connected across the power supply V_1 and V_2 respectively. The variation in current I_1 (cathode discharge current) and I_2 (anode discharge current) through the resistors R_1 and R_2 had been measured when the anode bias V_2 changes from 0–200 V. The experiment was conducted in a low vacuum with air as the working gas.

In the present study MADLs were produced in the following way. Glow discharge plasma was initially produced between cathode and chamber by keeping the cathode at very high negative bias of -700 V. Once a steady plasma is achieved, an electron current is then driven through plasma by applying a positive bias to anode electrode fixed at a distance of 300 mm from cathode. The application of positive bias leads the electrons to stream towards anode from cathode side in the background of stationary cold ions. At certain lower critical value of anode bias denoted as V_{LC}, a sudden rise of an instability cause the charges self-organize to form MADL with three alternate dark and bright regions having a cone-in-cone geometry forms as shown in Fig. 2 (multimedia view), the geometry of the structure including the diameter of the layers, number of layers were attributed to the length of the chamber, size of electrodes, separation between electrodes etc. The MADL with three successive layers remained till the anode voltage reaches an upper critical value (V_{UC}). Beyond this upper critical value, the MADL transform or decay into other MADL states with reduced number of layers and size. For very large value of, V_2, all the DLs vanish and completely transform into a highly intense anode glow (AG). The complete evolution of this triple DL including transition from triple to double, double to single, single to anode glow (AG) and reverse can be obtained by monotonically increasing and decreasing V_2 in the range of 0–200 V.

Three floating probes P_1, P_2, and P_3 fixed distance of 3 mm, 30 mm and 80 mm from anode and a Langmuir probe P_L were used to measure the floating potential and plasma parameters respectively. The floating probes were fixed in such a way that any two of the three probes will sit at opposite layer of charges of the MADL with variation in DL dimension for a change in either pressure or voltage as schematically shown in Fig. 1. The floating probes were also used to record the fluctuations in floating potential by connecting the floating probes to a Lecroy 500 MHz wavejet oscilloscope having a sample rate of 2 GS/s using high impedance passive probe (10 MΩ) with system attenuation of $10\times \pm 2\%$ to record the signal. More details about the experimental set-up can be found in [37].

3. Characteristics of MADL

In this section, we are focusing on two major characteristics of MADL in glow discharges mainly current–voltage characteristics and floating potential characteristics. Investigations carried out by Conde and Leon (1994) in constricted glow discharge [38] on the I–V characteristics revealed that discharge current, I_{dis} and discharge voltage, V_{dis} remain unaffected by the disappearance or upsurge of a new plasma corona or double layer. Later, role of discharge current in the number of plasma corona was studied by M. Strat [39] in a system consisting of two anodes and two cathodes revealed that the current was not steady rather consisted of regular spikes when there was a diffuse luminous plasma formation in front of anode. A sudden jump in current was observed when a nearly spherical intense luminous region with sharply defined boundaries was observed. It was concluded that double layer transforms into two, three or multiple DL structures when the cur-

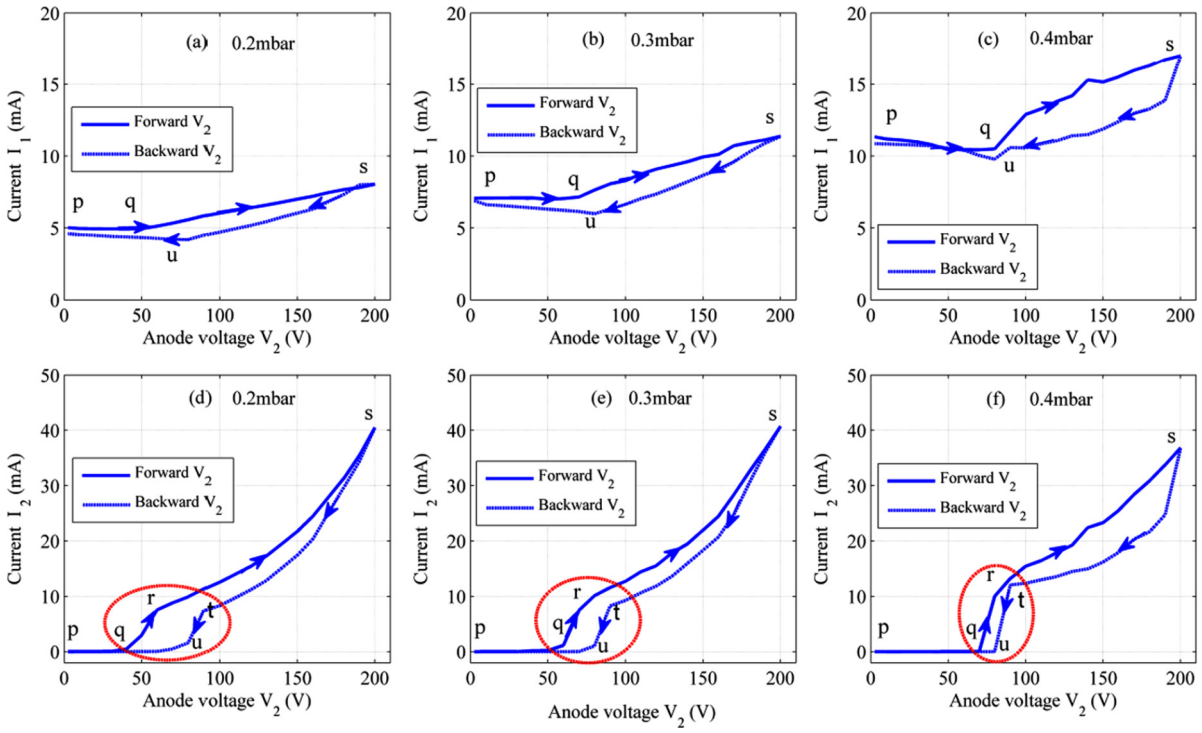

Fig. 3. The variation in current I_1 and I_2 across the resistors R_1 and R_2 with applied anode voltage V_2 has been shown. The figures in top row (a), (b) and (c) and bottom row (d), (e) and (f) represent V_2–I_1 and V_2–I_2 at pressure 0.2 mbar, 0.3 mbar and 0.4 mbar respectively. The solid and dashed line respectively represents the discharge current measured during the forward swing and backward swing of the anode voltage V_2.

rent collected by the electrode increased. When the voltage across the anode is decreased, the current–voltage characteristics show a hysteresis which follows an anti-clockwise direction. This phenomenon proves that DL can maintain their static or dynamic state for conditions weaker than those required for creation [40]. In this section, we present the current–voltage characteristics of MADL obtained in a different experimental setup when a reverse process takes place, i.e., MADL transforms into double DL, single DL and finally to intense anode glow, when the discharge current across the electrode increases. The corresponding hysteresis in I–V characteristics has a clockwise nature unlike from the previous reported results. The critical values required for the creation and maintenance of MADL under different experimental condition is also presented. In the next subsection we present how we characterized the MADL structure using floating probes which helps to understand the charge separation with in the MADL when the DL formed.

3.1. Current–voltage characteristics

The current collected by the electrodes under MADL formation was obtained across current limiting resistor R_1 and R_2. The current collected by the cathode is denoted as I_1 and that of anode is denoted as I_2. The corresponding current voltage characteristics are shown in Fig. 3. The upper row represents current–voltage characteristics obtained across cathode (V_2–I_1) and lower row shows characteristics obtained across anode (V_2–I_2) electrode. In Fig. 3(a), the critical values of V_2 are marked with points p, q, s and u, for pressure 0.2 mbar. The point p represents condition when $V_2 = 0$ V and the current, $I_1 = 5$ mA. The non-zero value of current obtained in the absence of anode voltage corresponds to the current carried by thermal electrons at the cathode. It remained constant up to the point q, $V_q = 40$ V. This voltage V_q is referred as lower critical voltage (V_{LC}) and at this voltage a three layered optically visible MADL appeared. On increasing V_2 MADL vanishes at $V_q = 60$ V, which is referred as upper critical voltage (V_{UC}). Beyond V_{UC}, the current I_1 keep on increasing linearly up to the point s, $V_s = 200$ V. At this voltage, only an intense anode glow is observed. Followed by backward swing of voltage, for which the current I_1 decreases linearly, with a different slope, up to the point u. At $V_u = 80$ V, it attained the initial value of $I_1 \sim 5$ mA and remained almost constant up to $V_2 = 0$ V. As shown in Fig. 3(a), (b) and (c), with increase in pressure, the minimum value of current I_1, for anode bias $V_2 = 0$ V, increases from 5 mA at 0.2 mbar to 13 mA at 0.4 mbar represents the increase of electron thermal current with increase in pressure. This small increase in current indicates that even though the seed electrons for the MADL formation was supplied from the glow discharge plasma at the cathode region, its contribution to the total current is significantly low compared to the anode current.

The corresponding V_2–I_2 characteristic obtained at 0.2 mbar is shown in Fig. 3(d). This figure is more informative and the critical values of V_2 have been marked with two more additional points namely r and t other than points p, q, s and u. With increasing V_2 from $V_2 = 0$ V, the current ($I_2 \sim 0$ mA) remained constant up to the point q. On further increasing V_2, the current I_2 increases explosively from $V_q = 40$ V to the point r, $V_r = 60$ V, of the order of ∼100 times the magnitude of electron thermal current. For the anode voltage above V_r, the MADL begins to decay (i.e. three layered MADL decays to two layered MADL and so on) though the current keeps on increasing exponentially but with lower growth rate up to the point s, $V_s = 200$ V. From $V_s = 200$ V, V_2 is swung backwards to 0 V. The current decreases exponentially up to the point t, $V_t = 90$ V, a three layered MADL reappeared again. On further reduction of anode voltage, the current decreases exponentially but with a steeper decay rate and at point u, $V_u = 80$ V, the MADL vanishes. This voltage V_u at which the MADL vanishes while downward swing of anode voltage corresponds to the minimum value of current $I_2 \sim 0$ mA. It can be noted from Fig. 3(d), (e) and (f) that as the pressure increases from 0.2 to 0.3 and to 0.4 mbar, the value of V_q increases to 40 V, 50 V and 70 V respectively. Similarly, the value of V_r also increases from 60 V to 70 V and

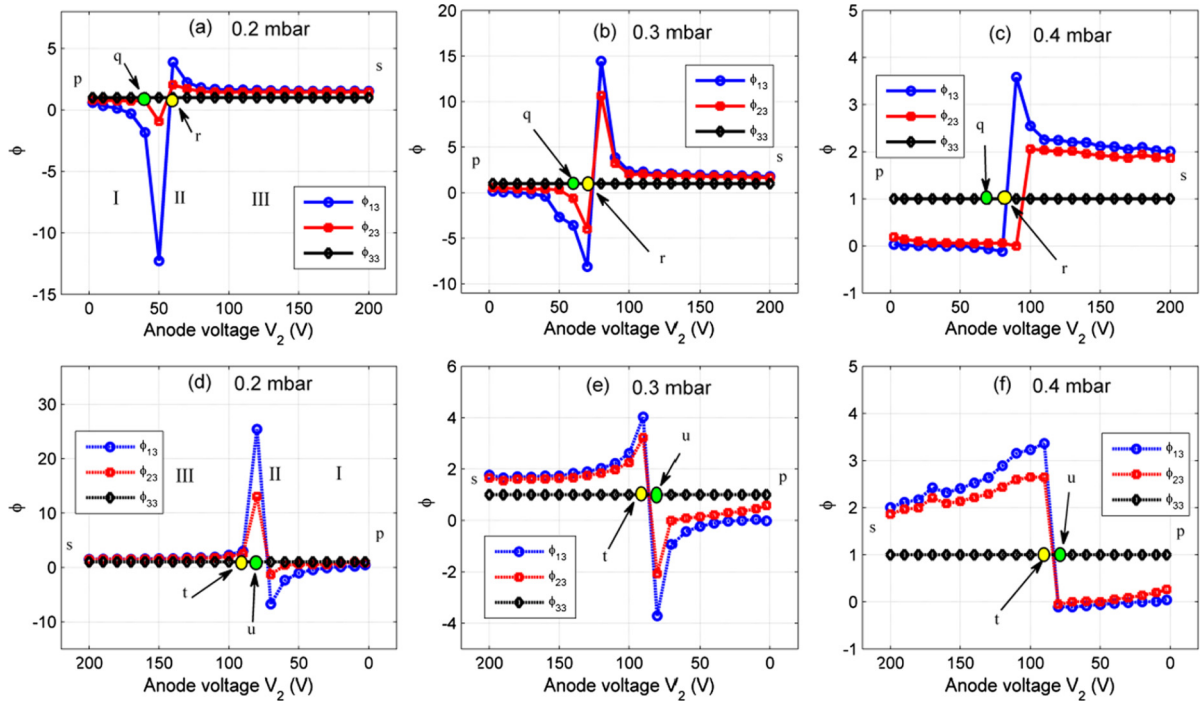

Fig. 4. Shows relative variation of floating potential (ϕ_{13}, ϕ_{23} and ϕ_{33}) measured by probes P_1, P_2 and P_3 with anode voltage V_2. The relative variations in all the plots are obtained with respect to measurements of probe P_3 (say $\phi_{13} = \phi_1/\phi_3$, $\phi_{23} = \phi_2/\phi_3$ and $\phi_{33} = \phi_3/\phi_3$). The figures in top row (a), (b) and (c) represents the floating potential measured for the forward swing of anode voltage V_2 and the bottom row (d), (e), (f) denotes the floating potential measured for the backward swing of V_2 for different pressure 0.2, 0.3 and 0.4 mbar.

to 80 V. However, the value of V_t and V_u remain unchanged for higher pressure. This is because with reduction in anode voltage, ionization as well as plasma density reduces as a consequence of reduction in number density of fast electrons in the EED [41–43]. When this tail has sufficiently low number density, sudden reduction in current occurs at point '*t*' which is independent of pressure. Where as in the forward swing, increase in pressure, electron-neutral collision mean free path reduces and to achieve ionization voltage must be increased to compensate this [41–43]. The V_2–I_2 characteristic indicates that a stable MADL structure consisting of three successive layers exist only between V_q and V_r in the forward swing of anode bias and V_t and V_u in the backward swing. As shown in the figure I_1 and I_2 traces different path in the forward and backward swing of anode voltage since the current collected by the electrodes in the forward swing of anode voltage is higher than that in the backward swing of V_2, which resulted in a clockwise hysteresis in discharge current–voltage characteristics. The sudden jump in discharge current at '*q*' and drop at '*t*' with the upsurge and disappearance of MADL indicate that the role of current related instability in the formation of MADL.

3.2. Comparison of special floating potential characteristics with in MADL

The floating potential characteristics of MADL were obtained using three electrostatic probes fixed at separate axial distance as described in sec. 2. Typically, DLs were characterized using movable biased probes to obtain the density and plasma potential along the axis of the DL. But MADLs in the present experiment was very sensitive to biased probes and characterization using movable probe completely disrupt the MADL structure itself. In this study MADLs were characterized by obtaining the variation in floating potential by placing probes within different layers of MADL as it emerges and decays. Then floating potential at the inner and outer layer of MADL was compared with floating potential outside the MADL as shown in Fig. 4 for a voltage range of 0–200 V. The floating potential measured by probe-1, 2 and 3 are denoted by ϕ_1, ϕ_2 and ϕ_3 and probe-1 and 2's variation with respect to probe-3 is denoted by ϕ_{13}, ϕ_{23} and ϕ_{33} (where $\phi_{13} = \phi_1/\phi_3$, $\phi_{23} = \phi_2/\phi_3$ and $\phi_{33} = \phi_3/\phi_3$). The figures in top row 4 (a), (b) and (c) presents variation in floating potential measured for the forward swing of anode voltage V_2 and the bottom row 4 (d), (e), (f) presents the floating potential measured for the backward swing of V_2 for different pressure 0.2, 0.3 and 0.4 mbar respectively. As shown in Fig. 4(a), at $V_2 = 0$ V, the floating potential measured by probes P_1 and P_2 is marginally negative with respect to P_3, representing typical potential measured across any floating substrate immersed in plasma. With increasing V_2, ϕ_{13} decreases exponentially, however, ϕ_{23} begins to decrease at $V_2 = V_q = 40$ V which corresponds to the value at V_q of the V_2–I_2 characteristics curve shown in Fig. 4. This change in ϕ_{13} and ϕ_{23} indicates that now the DL characteristics dominate over the floating substrate characteristics and $d\phi$ (variation in ϕ with respect to V_2) will have a nonzero value. As shown in figure, ϕ_{13} and ϕ_{23} both attained a minimum value at $V_2 = 50$ V (at pressure 0.2 mbar). On further increasing V_2 beyond 50 V the sign of ϕ_{13} and ϕ_{23} was reversed and attained a maximum value at $V_2 = V_r = 60$ V, followed by exponential decrease and thereafter it remained constant up to $V_2 = V_s = 200$ V. The reversal of sign indicates that with respect to probe-3, the probe-1 and probe-2 records different sets of space charge regions as the value of V_2 crosses 50 V. This field reversal nature is a key signature of the presence of DL consisting of two parallel regions having different charges. As shown in Figs. 4(b) and (c) for 0.3 mbar and 0.4 mbar, with increase in pressure, the characteristics of ϕ_{13} and ϕ_{23} is preserved. However, due to increase of plasma density with pressure, for 0.4 mbar, the value of ϕ_{13} and ϕ_{23} at $V_2 = 0$ V, and $V_2 = 200$ V is appreciably higher as shown in Fig. 4(c).

Furthermore, the anode voltage V_2 is swung backwards from 200 V to 0 V. At $V_2 = V_t = 90$ V, a 3 layered MADL reappeared and ϕ_{13} again attains the maximum value. This voltage is represented by the point V_t of the V_2–I_2 characteristics curve shown in Fig. 3. On further decreasing V_2 beyond V_t the sign of ϕ_{13}

and ϕ_{23} reversed and it attained once again a minimum value and MADL disappears at $V_u = 80$ V. As shown in Fig. 4(d) the ϕ_{13} and ϕ_{23} decay exponentially, however, remain marginally negative up to $V_s = 0$ V. From Fig. 4(e) and (f), with increase in pressure, the characteristics of ϕ_{13} and ϕ_{23} for backward swing of V_2, is preserved. However, the value of ϕ_{13} and ϕ_{33} for anode voltage $V_2 = 0$ V, and $V_2 = 200$ V is significantly larger at higher pressures. From the above observation, three regions can be identified from Fig. 4(a) region-I and III where variation in ϕ is constant and region-II where ϕ is varying towards the maxima and minima. The region II corresponds to a stable DL region where as in the region I and III, either DLs were not observed or DLs were in the decay stage leading towards anode glow, similarly for other figures. The maxima and minima of the floating potential shown in Fig. 4 corresponds to the opposite space charges of DL recorded by floating probe. The results showed that, in the present experimental condition, for a pressure range of 0.2 mbar to 0.4 mbar, DL existed only between the voltage range 40 V–80 V. This observation has been analyzed in the following section.

4. Results and discussion

The boundary conditions for the formation and existence and the role of Buneman instability in the triggering of MADL is analyzed in this section. The excitation of Buneman instability is established in the next subsection using the floating potential fluctuations recorded using floating probe.

4.1. Boundary conditions and Buneman instability

The current–voltage characteristics and floating potential characteristic reveals that MADL formation is associated with an instability and it exist between a certain range of anode voltage. In order to address this issues drift velocity and density of electrons were estimated under MADL conditions. At $V_2 = 40$ V, an explosive increase in current is observed, indicates that electrons have sufficient energy for ionization which is accompanied by simultaneous formation of visible MADL. At this voltage, the drift velocity exceeds a certain value of electron thermal velocity, ($v_d = 1.24 v_{te} = 1.17 \times 10^6$ m/s) which is exactly the threshold condition for Buneman instability given by Smith and Goertz ($v_d = 1.3 v_{te}$) and consequently electron density jumps from 5.64×10^{15} m^{-3} to 4.50×10^{16} m^{-3} i.e., ~7.5 times increases in density. Similar values of drift velocity were obtained for 0.3 and 0.4 mbar. These super thermal electrons cause Buneman instability and leads to formation of MADL by self-organization of space charges, the resultant current growth observed from the experiment is in agreement with this. The so formed potential structure of MADL consists of free/trapped electrons and ions. The electrons coming from lower potential side with energy ($m_e v_d^2$) greater than the MADL potential (ϕ) will reach the anode (free particles), i.e., $m_e v_d^2 \geq e\phi$, where as other electrons will not $m_e v_d^2 < e\phi$ (trapped particles). Similarly for the case of ions at the higher end of the potential.

Further increase of anode bias above 40 V, the number of free electrons with energy $m_e v_d^2$ greater than $e\phi$ has increased and consequently the number of free electrons arriving at the anode region has also increased. In order to satisfy the continuity equation there is a corresponding decrease in trapped electrons. At $V_2 = 60$ V, for 0.2 mbar, where the DL begins to decay, the calculated drift velocity was 2.99 v_{te}. The similar stage of the MADL for 0.3 mbar was observed at $V_2 = 70$ V and for 0.4 mbar, V_2 was between 80 V–90 V. The estimated value of drift velocity at 0.3 mbar was $2.99 v_{te}$ and it was between $0.77 v_{te}$ and $4.71 v_{te}$ for 0.4 mbar. The discrepancy in estimated values of drift velocity at 0.4 mbar arising from the experimental limitation. The experiment was carried out by increasing anode voltage with a step size of 10 V. Any value of drift velocity which falls within this limit was not calculated. The decay of the MADL above 60 V was resulted from this free and trapped particle imbalance. Beyond 60 V, an exponential growth in current is observed with electron drift velocity exceeds three times ($v_d \geq 3 v_{te}$) the electron thermal velocity. Therefore, mean energy of electron arrive at the anode zone increases above the ionization potential of the background gas, an intense ionization will take place and the MADL completely transformed into high intense anode glow. In brief, the explosive current growth at 40 V gives rise to the formation of MADL whereas the second exponential growth of current causes the decay of double layer and further to anode glow.

In the backward swing of anode bias from 200–0 V, the drift velocity remained almost same as that in the forward swing but number density of the electrons changed marginally. As an example, the number density of electrons at 40 V, for 0.2 mbar, where a triple MADL state is observed was $\sim 5.64 \times 10^{15}$ m^{-3} in the forward swing of V_2. Whereas in the backward swing of V_2, the same number density ($\sim 4.774 \times 10^{15}$ m^3) with same MADL state was observed at 70 V. This discrepancy arises from the difference in the electric field required to confine the charged species at the same V_2 in the forward and backward swing. The hysteresis observed with the MADL phenomenon is an outcome of this discrepancy. Unlike the previously reported anti-clockwise hysteresis in I–V characteristics, the present result shows a clockwise hysteresis indicating that same MADL state observed at a particular V_2 in the forward swing will appear at much higher values of V_2 in the backward swing. With increase in pressure the jumps in density associated with MADL also increases. As the pressure increased from 0.2 mbar to 0.4 mbar, the density at V_q and V_r increased from 5.64×10^{15} m^{-3} and 4.50×10^{16} m^{-3} to 2.27×10^{14} m^{-3} and 4.96×10^{16} m^{-3} respectively.

The results show that MADL appeared at a critical value of anode voltage, when electron drift velocity (v_d) and electron thermal velocity (v_{te}) are related by $v_d \geq 1.3 v_{te}$. Stable DLs were not observed for condition when $v_d \geq 3 v_{te}$. The analysis establishes a well-defined lower and upper limit of applied anode voltage, for the existence of MADL, i.e. between 40 V–80 V for a pressure range of 0.2 mbar to 0.4 mbar and provides an existence criteria in terms of drift velocity. This results are consistent with the Buneman instability condition given by smith and Goertz in numerical studies and upper limit of ordinary DL condition given by Quon and Wong.

4.2. Analysis of floating potential fluctuations and establishment of Buneman instability

The necessary condition for the formation of DL is that a strong electron current must pass through the plasma towards the higher end of the potential. It was first discussed by Langmuir while studying cathode double layer. He observed that for the formation of cathode double layer, electron density must decrease slower than the ion density as they move towards center of the layer from the cathode side and the ion density must decrease slower than electrons on the other side of the layer. This gives rise to the requirement of minimum value of velocity for ions and electron as given by Bohm criteria., i.e., the electron current must move with super thermal speed towards the anode side. In the present study, the estimated electron drift velocity for the triggering of MADL was $v_d = 1.3 v_{te}$, which is exactly the condition for the development of Buneman instability as discussed in sec. 4.1. To confirm the role of Buneman instability in the triggering of MADL, nonlinear oscillations excited during this stage were recorded and analyzed. These oscillations are 1 ms time traces of fluctuations in floating potential obtained using probe, P_1. Oscillations are recorded for every 10 V in the range $V_2 = 0$ V to $V_2 = 60$ V i.e., which

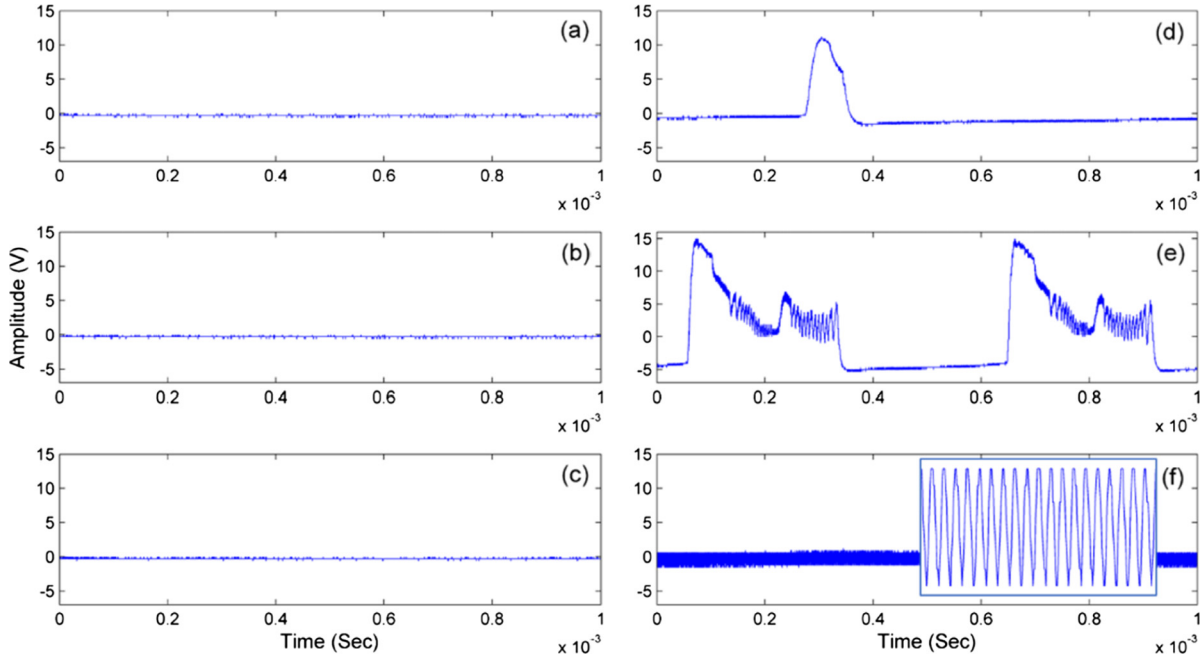

Fig. 5. Fluctuations in floating potential obtained for different values of anode voltage (a) 10 V, (b) 20 V, (c) 30 V, (d) 40 V, (e) 50 V and (f) 60 V. Enlarged version of oscillation in (f) is shown in the inset.

include MADL formation at $V_2 = 40$ V ($v_d = 1.3v_{te}$) till it begins to decay when $v_d \geq 3v_{te}$, are shown in Fig. 5. Even though electrons begin to stream towards the higher end of the potential as the anode bias was increased from a very small value of zero, no oscillations were excited till $V_2 = 40$ V as shown in Fig. 5(a) to (c). At $V_2 = 40$ V, sudden rise of a non-oscillatory potential in the form of a pulse is observed as shown in Fig. 5(d). This stage corresponds to an exponential jump in anode discharge current marked with '*r*' in the current–voltage characteristics. The amplitude of this 120 μS duration pulse was 11.2 V with a frequency of ∼2 KHz. At $V_2 = 50$ V, the potential structure bifurcates into a pulse consisting of more number of spectral complaints and the amplitude increases to the maximum value of ∼15 V with a time duration of 300 μS. At 60 V, the amplitude growth saturates and the instability collapse followed by a sudden drop in amplitude to ∼1 V with simultaneous decay of MADL. The oscillations at this stage is transformed into a high frequency sinusoidal oscillation with a frequency of ∼1 MHz.

The growth and collapse of instability observed during this process was a consequence of nonlinear evolution of Buneman instability as given by Galeev et al. [36]. Buneman instability is a special type of two stream instability arises when the entire electron population is steaming with respect to the ions in cold unmagnetized plasma. Numerical simulation carried out by Degroot et al. [44] and later by Belova et al. [45], Sigov [46] obtained similar correlation between DL and Buneman instability and showed that formation of potential spikes and its evolution into double layer is a consequence of nonlinear evolution of Buneman instability. Galeev et al. numerically estimated that this amplitude grows to a maximum of $e\varphi \max = (5 \text{ to } 6) \times \text{Te}$ until there is reflection of electrons from the potential minimum or the growth of the amplitude is limited to the initial energy of the electron current $e\varphi \max = 3/2 m_e v_d^2$. From the experiment, at $V_2 = 40$ V, the estimated initial energy of the electron was ∼12 V, which gives a good approximation to the maximum potential 15 V observed at $V_2 = 50$ V. The growth at 50 V was limited by the electrons reflected from the minimum of the potential. Recent simulation agree with the fact that Buneman DLs decay either by the formation of shock when the DL potential is maximum which drive of the instability by reflection of electrons from the minimum of the potential or by the emission of solitons propagating in the downstream direction which carry energy away from the DL in the case of ion acoustic DL [47,48]. This large number of reflected electrons leads to the disappearance of region of negative potential followed by the collapse of instability, which is consistent with observation made in Fig. 4(a) region-II where a region of negative potential vanishes beyond 60 V. The experimental results are consistent with numerical simulation results for the nonlinear evolution of Buneman instability and DL formation.

5. Conclusions

We summarize the important results of present investigation. In this study, we have generated multiple anodic double layers in dc glow discharge plasma with separate power supplies for the anode and cathode. The streaming of electrons towards the anode is controlled by applied anode voltage. At a critical anode voltage (V_{LC}), Buneman instability is triggered which is observed by sudden rise of floating potential and simultaneous formation of MADL. Spatial floating potential variation with in the MADL structure were obtained using three electrostatic probes fixed at different location along the axis of MADL. Analysis of variations in floating potentials, reversal of potential obtained at different location along the axis, confirmed the existence of MADL. The lower critical voltage (V_{LC}) is consistent with the condition required for existence of Buneman instability, that is, electron drift velocity (v_d) and electron thermal velocity (v_{te}) are related by $v_d \geq 1.3v_{te}$. In addition to this, we also obtained an upper critical voltage (V_{UC}) for existence of MADL. Therefore, the main outcome of this investigation is observation of boundary condition $3v_{te} \geq v_d \geq 1.3v_{te}$ for existence of MADL. Furthermore, floating potential fluctuation confirmed that triggering of Buneman instability is associated with sudden growth of nonoscillatory potential, which coincides (V_{LC}). On further increase of anode voltage, the amplitude of instability grows and finally bifurcates, at upper critical voltage (V_{UC}), and the instability collapses into sinusoidal periodic oscillation of low amplitude. This observation is consistent with existing formalism of Buneman instability leading to formation of DLs.

Acknowledgements

This work is partially supported by UGC-MRP (grant F.NO41-970/2012(SR)), DST-FTP Government of India (grant SR/FTP/PS-053/2010) and Start-Up Grant received from Pondicherry University.

References

[1] L.P. Block, Astrophys. Space Sci. 55 (1978) 59.
[2] P. Carlqvist, in: P. Michelsen, J.J. Rasmussen (Eds.), Proc. Symposium on Plasma Double Layers, 1982.
[3] J.S. Wagner, T. Tajima, J.R. Kan, J.N. Leboeuf, S.I. Akasofu, J.M. Dawson, Phys. Rev. Lett. 45 (1980) 803.
[4] J.E. Borovsky, Phys. Rev. Lett. 69 (1992) 1054.
[5] D.S. Main, D.L. Newman, R.E. Ergun, Phys. Rev. Lett. 97 (2006) 185001.
[6] F.S. Mozer, O.V. Agapitov, A. Artemyev, J.F. Drake, V. Krasnoselskikh, S. Lejosne, I. Vasko, Geophys. Res. Lett. 42 (2015) 3627–3638.
[7] R. Boström, G. Gustafsson, B. Holback, G. Holmgren, H. Koskinen, P. Kintner, Phys. Rev. Lett. 61 (1988) 82.
[8] C.K. Goertz, G. Joyce, Astrophys. Space Sci. 32 (1975) 165.
[9] D.S. Main, D.L. Newman, C. Scholz, R.E. Ergun, Geophys. Res. Lett. 40 (2013) 2897–2901.
[10] R.E. Ergun, Y.J. Su, L. Andersson, C.W. Carlson, J.P. McFadden, F.S. Mozer, D.L. Newman, M.V. Goldman, R.J. Strangeway, Phys. Rev. Lett. 87 (2001) 045003.
[11] R.A. Smith, Phys. Scr. 25 (2) (1982) 413–415.
[12] N. Singh, Plasma Phys. 24 (1982) 639.
[13] K. Goswamy, K.S. Saharia, H. Schamel, Phys. Plasmas 15 (2008) 062111.
[14] L.P. Block, Cosm. Electrodyn. 3 (1972) 349.
[15] G. Knorr, C.K. Goertz, Astrophys. Space Sci. 31 (1974) 209–223.
[16] N. Singh, S.M. Loo, B.E. Wells, C. Deverapalli, Geophys. Res. Lett. 27 (2000) 927.
[17] N. Hershkowitz, Space Sci. Rev. 41 (1985) 351–394.
[18] C. Charles, Plasma Sources Sci. Technol. 16 (2007) R1–R25.
[19] P. Coakley, N. Hershkowitz, Phys. Fluids 22 (1979) 1171.
[20] P. Leung, A.Y. Wong, B.H. Quon, Phys. Fluids 23 (1980) 992.
[21] J.M. Griffin, A.C. Forse, W.Y. Tsai, P.L. Taberna, Nat. Mater. 14 (2015) 812.
[22] C.A. Helm, J.N. Israelachvii, P.M. Mcguiggan, Science 246 (1989) 919.
[23] H.P. Fernandes, C.L. Cesar, M.L. de Castro, Rev. Bras. Hematol. Hemoter. 33 (4) (2011) 297–301.
[24] N. Singh, R.W. Schunk, Geophys. Res. Lett. 9 (1982) 12.
[25] R.A. Smith, C.K. Goertz, J. Geophys. Res. Space Phys. 83 (A6) (1978) 2617–2627.
[26] M. Temerin, K. Cerny, W. Lotko, F.S. Mozer, Phys. Rev. Lett. 48 (1982) 17.
[27] T. Sato, H. Okuda, Phys. Rev. Lett. 49 (1980) 740.
[28] A. Bailey III, N. Hershkowitz, Geophys. Res. Lett. 15 (1988) 99–102.
[29] D.G. Dimitriu, M. Aflori, L.M. Ivan, V. Radu, E. Poll, M. Agop, Plasma Sources Sci. Technol. 22 (2013) 035007.
[30] S.D. Baalrud, B. Longmier, N. Hershkowitz, Plasma Sources Sci. Technol. 18 (2009) 035002.
[31] L. Conde, C. Ferro Fontán, J. Lambás, Phys. Plasmas 13 (2006) 113504.
[32] Bengt Hultqvist, Scientific Results from the Swedish Viking Satellite, Status Report, Swedish Inst. of Space Physics, Kiruna, 1988.
[33] M.H. Boehm, F.S. Mozer, An S3-3 search for confined regions of large parallel electric fields, Geophys. Res. Lett. 8 (6) (1981) 607–610.
[34] R. Pfaff, C. Carlson, J. Watzin, D. Everett, T. Gruner, An overview of the Fast Auroral SnapshoT (FAST) satellite, Space Sci. Rev. 98 (1) (2001) 1–32.
[35] B.H. Quon, A.Y. Wong, Phys. Rev. Lett. 37 (1976) 1393.
[36] A.A. Galeev, R.Z. Sagdeev, V.D. Shapiro, V.I. Shevchenko, Sov. Phys. JETP 54 (2) (1981).
[37] P. Alex, A. Saravanan, K. Jayaprakash, K.S. Suraj, Results Phys. 5 (2015) 235–240.
[38] L. Conde, L. Leon, Phys. Plasmas 1 (1994) 2441.
[39] M. Strat, Georgeta Strat, S. Gurlui, Phys. Plasmas 10 (2003) 3592.
[40] S. Chiriac, D.G. Dimitriu, M. Sanduloviciu, Phys. Plasmas 14 (2007) 072309.
[41] Brian Chapman, Glow Discharge Process, Wiley–Interscience Publication, 1980.
[42] Yuri P. Raizer, Gas Discharge Physics, Springer-Verlag, 1991.
[43] Michael A. Lieberman, Allan J. Lichtenberg, Principles of Plasma Discharge and Material Processing, John Wiley & Sons, Inc., 2005.
[44] S. DeGroot, C. Barnes, A.E. Walsted, O. Buneman, Phys. Rev. Lett. 38 (1987) 1283.
[45] N.G. Belova, A.A. Galeev, R.Z. Sagdeev, Y.S. Sigov, JETP Lett. 31 (1980) 518–522.
[46] Y.S. Sigov, Phys. Ser. 2 (1982) 367.
[47] T.C. Li, J.F. Drake, M. Swisdak, Astrophys. J. 778 (2013) 144.
[48] T. Sato, H. Okuda, J. Geophys. Res. 86 (A5) (1981) 3357–3368.